Protein Phosphatase 1 Inhibitor-1 Deficiency Reduces Phosphorylation of Renal NaCl Cotransporter and Causes Arterial Hypotension

Nicolas Picard,*[†] Katja Trompf,* Chao-Ling Yang,[‡] R. Lance Miller,[§] Monique Carrel,* Dominique Loffing-Cueni,* Robert A. Fenton,[∥] David H. Ellison,[‡] and Johannes Loffing*

*Institute of Anatomy, University of Zurich, Zurich, Switzerland; [†]Paris Cardiovascular Research Center, Institut National de la Santé et de la Recherche Médicale Unit 970, Université Paris-Descartes, Paris, France; [‡]Department of Medicine, Oregon Health and Science University, Portland, Oregon; [§]National Heart Lung Blood Institute, National Institutes of Health, Bethesda, Maryland; and [∥]Department of Biomedicine, Aarhus University, Aarhus, Denmark

ABSTRACT

The thiazide-sensitive NaCl cotransporter (NCC) of the renal distal convoluted tubule (DCT) controls ion homeostasis and arterial BP. Loss-of-function mutations of NCC cause renal salt wasting with arterial hypotension (Gitelman syndrome). Conversely, mutations in the NCC-regulating WNK kinases or kelch-like 3 protein cause familial hyperkalemic hypertension. Here, we performed automated sorting of mouse DCTs and microarray analysis for comprehensive identification of novel DCT-enriched gene products, which may potentially regulate DCT and NCC function. This approach identified protein phosphatase 1 inhibitor-1 (I-1) as a DCT-enriched transcript, and immunohistochemistry revealed I-1 expression in mouse and human DCTs and thick ascending limbs. In heterologous expression systems, coexpression of NCC with I-1 increased thiazide-dependent Na^+ uptake, whereas RNAi-mediated knockdown of endogenous I-1 reduced NCC phosphorylation. Likewise, levels of phosphorylated NCC decreased by approximately 50% in I-1 (I-1$^{-/-}$) knockout mice without changes in total NCC expression. The abundance and phosphorylation of other renal sodium-transporting proteins, including NaPi-IIa, NKCC2, and ENaC, did not change, although the abundance of pendrin increased in these mice. The abundance, phosphorylation, and subcellular localization of SPAK were similar in wild-type (WT) and I-1$^{-/-}$ mice. Compared with WT mice, I-1$^{-/-}$ mice exhibited significantly lower arterial BP but did not display other metabolic features of NCC dysregulation. Thus, I-1 is a DCT-enriched gene product that controls arterial BP, possibly through regulation of NCC activity.

The distal convoluted tubule (DCT) plays a pivotal role in the renal control of ion homeostasis and BP.[1] The DCT reabsorbs approximately 10% of the filtered NaCl load and is significantly involved in renal potassium (K^+), calcium, magnesium, and acid/base handling.[1] The thiazide-sensitive NaCl cotransporter (NCC) is the major apical sodium (Na^+) transport pathway in the DCT. In the late DCT, NCC abundance overlaps with the expression of the epithelial sodium channel (ENaC), which is the apical sodium reabsorption pathway in the connecting tubule and collecting duct. NCC activity and hence, DCT salt transport are regulated by a variety of factors, including dietary ion intake, plasma

hormones (*e.g.*, aldosterone, angiotensin II, and vasopressin), and metabolic factors (*e.g.*, alkalosis).[1,2] Several human tubulopathies (genetic and acquired) have been attributed to dysfunctions of

the DCT. Loss-of-function mutations of NCC (Gitelman syndrome) cause renal salt wasting with hypotension, hypokalemic alkalosis, and hypocalciuria,[3] whereas increased NCC activity because of mutations within the NCC-regulating with-no-lysine kinase 1 (WNK1) or WNK4 (familial hyperkalemic hypertension) are associated with severe salt-sensitive hypertension, hyperkalemia, metabolic acidosis, and hypercalciuria.[4] Increased NCC expression has been linked to renal Na^+ retention in liver cirrhosis,[5] diabetes mellitus,[6] β-adrenergic stimulation,[7] and immunosuppressive treatment.[8] The clinical significance of the DCT is also emphasized by clinical trials that confirmed the DCT as an important target for antihypertensive therapy.[9]

The identification of the WNKs as regulators of NCC[4] was key for our current understanding of the molecular mechanisms that control NCC. WNK1 and WNK4 are serine/threonine kinases that interact in a complex cascade with the STE20-related proline-alanine-rich kinase (SPAK) to regulate NCC phosphorylation (e.g., Thr44, Thr53, Thr58, and Ser71 in mouse NCC) and finally, activity.[8,10–12] In addition to the WNK–SPAK pathway, several other proteins were identified to control NCC, including parvalbumin (PV),[13] serum and glucocorticoid-inducible kinase Sgk1, ubiquitin ligase Nedd4–2,[14–16] kelch-like 3 (KLHL3),[17,18] cullin 3,[17,18] and protein phosphatase (PP) 4.[19]

Remarkably, several of the above listed regulatory proteins are highly abundant in the DCT (e.g., WNK4, KS-WNK1, SPAK, PV, and KLHL3). Therefore, we hypothesized that the DCT may express a particular set of DCT-enriched gene products, of which at least some participate in the regulation of NCC-mediated sodium absorption. Encouraged by previous gene expression analysis on freehand-isolated renal tubules in the works by Chabardès-Garonne et al.,[20] Cheval et al.,[21] and Pradervand et al.,[22] we aimed at identifying DCT-enriched gene products using a transcriptomic approach. We used complex object parametric analysis and sorting (COPAS) of renal tubules, which was developed by Miller et al.,[23] to isolate DCTs on a large scale. Among others, we identified the PP1 inhibitor-1 (I-1) to be highly enriched in the DCT. I-1 is encoded by the Ppp1r1a gene and forms a small, 171-aa-long cytosolic protein[24] that was the first identified endogenous inhibitor of PP1.[25] Here we show that I-1 affects the phosphorylation of NCC in vitro and in vivo. I-1 deficiency reduces NCC phosphorylation and lowers arterial BP in mice.

RESULTS

Identification of DCT-Enriched Genes
For large-scale isolation of mouse DCTs by COPAS, we used a transgenic mouse model expressing the enhanced green fluorescent protein (EGFP) under the control of the PV promoter (PV-EGFP).[26] Immunofluorescent labeling of kidney cryosections from these mice confirmed the orthotopic expression of EGFP in the PV-positive early DCTs but not the

ENaC-positive late DCTs (Figure 1, A and B). Kidneys of these mice were digested with collagenase and processed for COPAS as described in Concise Methods. Fluorescent emission and time of flight (as an indicator of tubule size) for each tubule fragment were plotted (Figure 1C). A selection window for sorting was set to collect three separate fractions, namely EGFP-positive tubules ($EGFP^+$), EGFP-negative tubules ($EGFP^-$), and all types of tubules (ALL) (Figure 1C). Subsequent analysis of gene expression and protein abundance confirmed a strong enrichment of DCT cells in the $EGFP^+$ samples (Figure 1, D and E). The DCT-specific NCC was highly enriched in the $EGFP^+$ samples compared with all tubules, whereas markers for proximal tubules (sodium-dependent phosphate cotransporter IIa [NaPi-IIa]), thick ascending limbs (sodium-potassium-2-chloride cotransporter-2 [NKCC2]), and connecting tubules and collecting ducts (AQP2) were almost absent from the $EGFP^+$ fraction. The weak band for βENaC (Figure 1E) likely relates to slight contaminations of early DCT samples, with attached late DCTs expressing βENaC.[27]

To identify DCT-enriched gene products, we performed comparative transcriptome analysis of sorted $EGFP^+$, $EGFP^-$, and ALL fractions using Whole Mouse Genome Microarrays (Agilent Technologies). $EGFP^+$/ALL and ALL/$EGFP^-$ expression ratios were determined for each gene product. The known DCT markers PV,[27] transient receptor potential-melastatin 6 (TRPM6),[28] and NCC[29] are strongly enriched in $EGFP^+$ samples but absent from the $EGFP^-$ samples (Supplemental Table 1). In contrast, gene expression for proximal tubule markers, such as aquaporin-1, NaPi-IIa, and megalin, was almost absent in the $EGFP^+$ fraction compared with the ALL tubule sample (Supplemental Table 1). To define DCT-enriched genes, the $EGFP^+$/$EGFP^-$ ratio was calculated for each gene. The 100 genes with the most prominent DCT enrichment are presented in Supplemental Table 2.

Among these genes, we found known regulators of NCC, such as PV,[13] KLHL3,[17,18] and WNK1,[30] with $EGFP^+$/$EGFP^-$ ratios of 935, 36, and 35, respectively (Supplemental Table 2). Although not among the first 100 gene products, WNK4 and SPAK are also significantly enriched in the $EGFP^+$ versus $EGFP^-$ fraction (ratios of 22 and 13, respectively). We then analyzed the list specifically for gene products that may interact with or counterbalance the action of these kinases. In this regard, I-1, which is markedly enriched ($EGFP^+$/$EGFP^-$ ratio of 47) in DCT, was found to be an interesting candidate.

I-1 Is Localized in the DCT and Thick Ascending Limb
Immunoblotting (IB) with an I-1 antibody confirmed the expression of I-1 at the protein level in kidneys of wild-type (WT) but not I-1$^{-/-}$ mice (Figure 2A). The specific band of the expected size of 28 kDa was very strong in sorted $EGFP^+$ tubules of WT mice, weak in $EGFP^-$ tubules, and moderate in all tubule samples consistent with a significant enrichment of I-1 in DCTs (Figure 2B). Immunohistochemistry (IHC) revealed several I-1–positive renal tubules in the renal cortex of
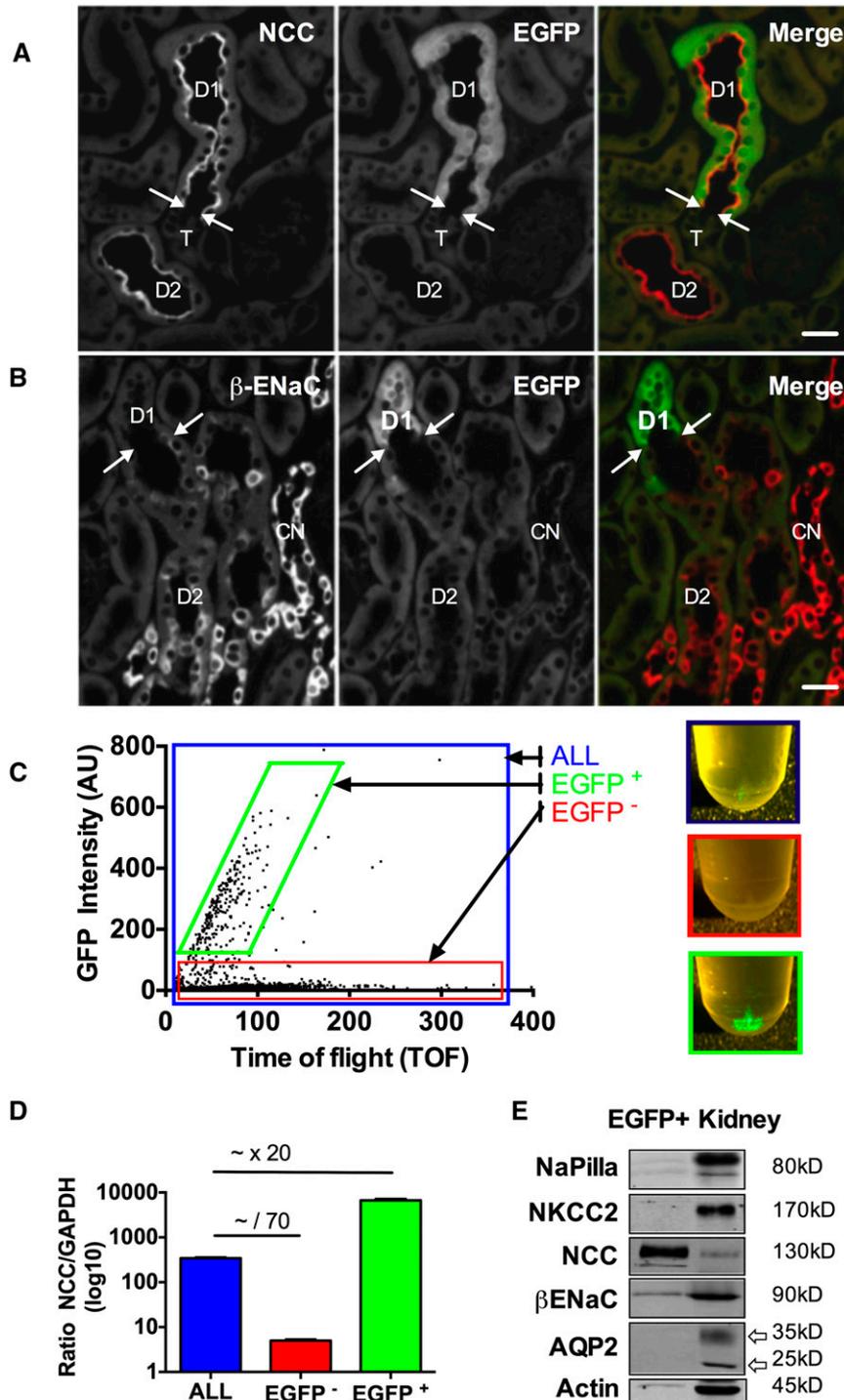
Figure 1. COPAS allows efficient isolation of EGFP-expressing DCTs. (A and B) Representative immunostainings of renal cryosections from PV-EGFP mice stained for (A) NCC or (B) βENaC. The EGFP signal colocalizes with NCC-positive early DCT (DCT1–D1) but not ENaC-positive late DCT (DCT2–D2), and ENaC-positive connecting tubules (CNs). Arrows indicate the transitions (A) from TAL (T) to D1 and (B) from D1 to D2. (C) EGFP⁺ tubules were sorted using COPAS. Fluorescent emission and relative size (measured by an axial light loss detector and called time of flight) were measured for each tubular segment from the tubular suspension. A selection window for sorting was set to collect EGFP⁺ (green), EGFP⁻ (red), or ALL (blue) tubules. Representative pellets for sorted 400 tubules for each fraction are shown in

WT but not I-1^{−/−} mice (Figure 2C). Detailed analysis of consecutive cryosections stained with antibodies against I-1, NCC, and calbindin D28k (CB28K) showed that I-1 protein is highly abundant in the cytoplasm of NCC- and CB28K-positive DCT cells. I-1 is also abundant in the preceding cortical (Figure 2D) and medullary thick ascending limb (TAL) (not shown). A similar distribution pattern was revealed in human kidneys (Supplemental Figure 1).

I-1 Regulates NCC Phosphorylation

To test the possible role of I-1 in controlling NCC phosphorylation, I-1 RNA interference knockdown experiments were performed in human embryonic kidney (HEK) cells stably expressing NCC[8] (Figure 3A). We first showed that HEK cells exhibit endogenous I-1 and its target PP1. Knockdown of I-1 by small interfering RNA substantially reduced the abundance of NCC phosphorylated at Thr53 but not the total abundance of NCC. These results suggest that I-1 is part of a novel pathway controlling NCC phosphorylation. To test for functional effects, we injected *Xenopus* oocytes with cRNAs encoding NCC together with PP1a, the catalytic subunit of PP1, or a constitutively active variant of I-1 (T35D).[31] I-1 (T35D) substantially increased ²²Na uptake (Figure 3B). PP1a slightly reduced ²²Na uptake, but the differences did not reach statistical significance. The heterologous overexpression of PP1a may not have been sufficient to overcome the known high activity of endogenous PP1 in the oocyte.[32]

To confirm that I-1 can exert similar effects *in vivo*, we analyzed NCC phosphorylation in kidneys of WT and I-1^{−/−} mice using antibodies against total NCC and

tubes in the right panel. (D) NCC gene expression levels were assessed by real-time PCR for EGFP⁺, EGFP⁻, and ALL tubules samples (n=4 mice). (E) Immunoblots of EGFP⁺ tubules (400 tubules/lane) and kidney lysates detecting NCC, βENaC, and other nephron segments markers (*i.e.*, NaPi-IIa, proximal tubule; NKCC2, thick ascending limb; AQP2, connecting tubule/collecting duct) confirmed the strong enrichment of NCC-positive DCTs in EGFP⁺ tubules. GAPDH, glyceraldehyde-3-phosphate dehydrogenase.
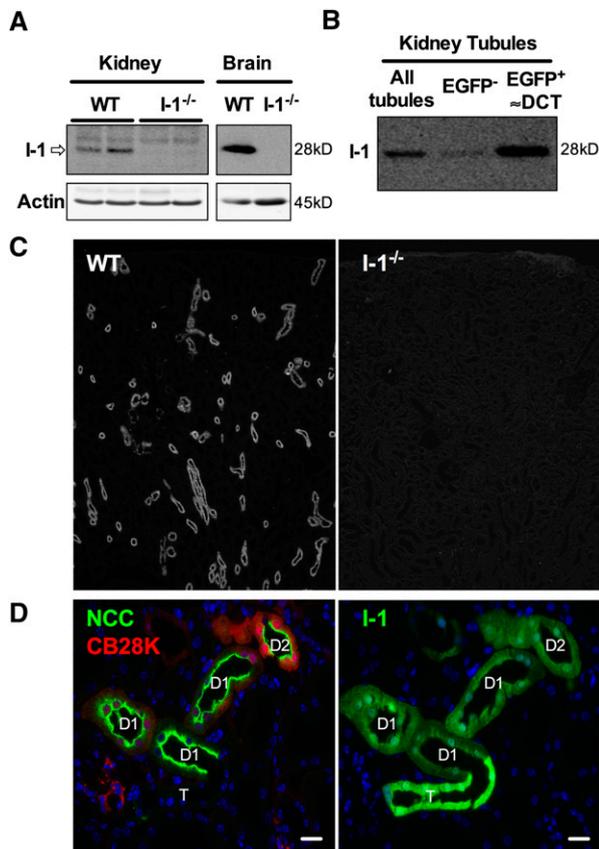
Figure 2. I-1 is highly abundant in mouse DCT and TAL. (A) Immunoblot analysis for I-1 in kidney and brain lysates from WT and I-1$^{-/-}$ mice. A band of the expected size (28 kD) is detected in kidney and brain of WT mice but not I-1$^{-/-}$ mice. Actin is used as a loading control. (B) Immunoblot analysis of COPAS-sorted tubules (400 tubules for each lane) for the nonselected (all tubules), EGFP$^-$, and EGFP$^+$ tubule fractions shows significant enrichment of I-1 in the EGFP$^+$ tubules. (C) Immunohistochemistry reveals I-1 in kidney tubules of WT but not I-1$^{-/-}$ mice. (D) Immunostaining of consecutive cryosections from WT mice shows a cytoplasmic I-1 localization in NCC- and CB28K-positive early DCTs (D1; no or weak CB28K) and late DCTs (D2; strong CB28K) and in the NCC-negative TAL (T). Scale bars, ~20 μm.

NCC phosphorylated at Thr53, Thr58, Ser71, and Ser89.[33] Similar to the results in HEK293 cells, total NCC abundance was similar in WT and I-1$^{-/-}$ kidneys, whereas the phosphorylation of NCC at all analyzed phosphorylation sites was significantly reduced (Figure 3, C and D).

Lower BP in I-1$^{-/-}$ Mice

NCC plays an important role in BP regulation, which is evidenced by high or low BP in mice with activated or suppressed NCC, respectively.[2,11,12] Therefore, we hypothesized that I-1 deficiency should lower BP. Indeed, I-1$^{-/-}$ mice have significantly lower systolic BP than WT mice on both standard (0.8% Na$^+$) and low Na$^+$ (0.05% Na$^+$) diets (Figure 4A).

I-1$^{-/-}$ Mice Manifest Features of Mild NCC Deficiency

To determine whether I-1$^{-/-}$ mice exhibit metabolic features suggesting NCC dysfunction, we performed metabolic studies. On standard diet, blood ion concentrations, blood pH, blood bicarbonate, and urinary ion excretion rates were similar to the values in WT mice (Tables 1 and 2). Likewise, plasma aldosterone levels and urinary aldosterone excretion were similar for WT and I-1$^{-/-}$ mice. Even on a low Na$^+$ diet, I-1$^{-/-}$ mice could rapidly reduce their urinary Na$^+$ excretion (Figure 4B), and urinary ion and aldosterone excretion did not differ between genotypes, even after 14 days of Na$^+$ restriction (Table 2). Nevertheless, on both standard and low Na$^+$ diets, I-1–deficient mice tended to have lower plasma K$^+$ levels than WT mice. NCC$^{-/-}$ mice must be challenged with dietary K$^+$ deprivation to exhibit frank hypokalemia.[34] Therefore, we fed WT and I-1$^{-/-}$ mice a low K$^+$ diet (0.05% K$^+$) for 4 days. In contrast to the NCC$^{-/-}$ mice,[34] I-1$^{-/-}$ mice were able to reduce urinary K$^+$ excretion similar to WT mice (Figure 4C). Plasma K$^+$ values remained lower in I-1$^{-/-}$ than WT mice, but differences still did not reach statistical significance (Figure 4D). To further test for the *in vivo* activity of NCC, we performed a hydrochlorothiazide (HCTZ) test. WT and I-1$^{-/-}$ mice were injected with either vehicle or HCTZ; urinary Na$^+$ excretion was measured for the subsequent 6 hours and expressed as the differences between thiazide- and vehicle-induced natriuresis. Statistical differences between genotypes were not detected on either standard or low Na$^+$ diet (Figure 4E). Nevertheless, on low Na$^+$ diet, I-1$^{-/-}$ mice had a tendency for a decreased HCTZ response ($P=0.08$ unpaired t test, WT versus I-1$^{-/-}$).

Compensatory Upregulation of Pendrin in I-1$^{-/-}$ Mice

To test whether upregulation of other ion transport pathways may compensate for reduced NCC phosphorylation and activity, we analyzed the abundance of several Na$^+$ transporting proteins expressed along the nephron (Figure 4F, Supplemental Table 3). The abundance of the NaPi-IIa of proximal tubules, the NKCC2 of thick ascending limbs, and the ENaC and the sodium-driven bicarbonate-chloride exchanger of principal and intercalated cells in the renal collecting system (*i.e.*, connecting tubule and collecting duct) were not altered in kidneys of WT versus I-1$^{-/-}$ mice. However, pendrin, the apical bicarbonate-chloride exchanger in nontype A intercalated cells, was found to be more abundant in kidneys of I-1$^{-/-}$ than WT mice (Figure 4F, Supplemental Table 3).

I-1 Deficiency Does Not Affect NKCC2 Phosphorylation

Because I-1 is also expressed in the TAL and because NKCC2 is homologous to NCC, we looked more specifically to the effect of I-1 deficiency on NKCC2 in an additional set of mice. By IB and IHC, we could not detect any significant differences between WT and I-1$^{-/-}$ mice for the abundance and subcellular localization of total NKCC2 and phospho-NKCC2 (Figure 5, A–C). To further exclude any downregulation of NKCC2, we performed a furosemide test. Interestingly, the
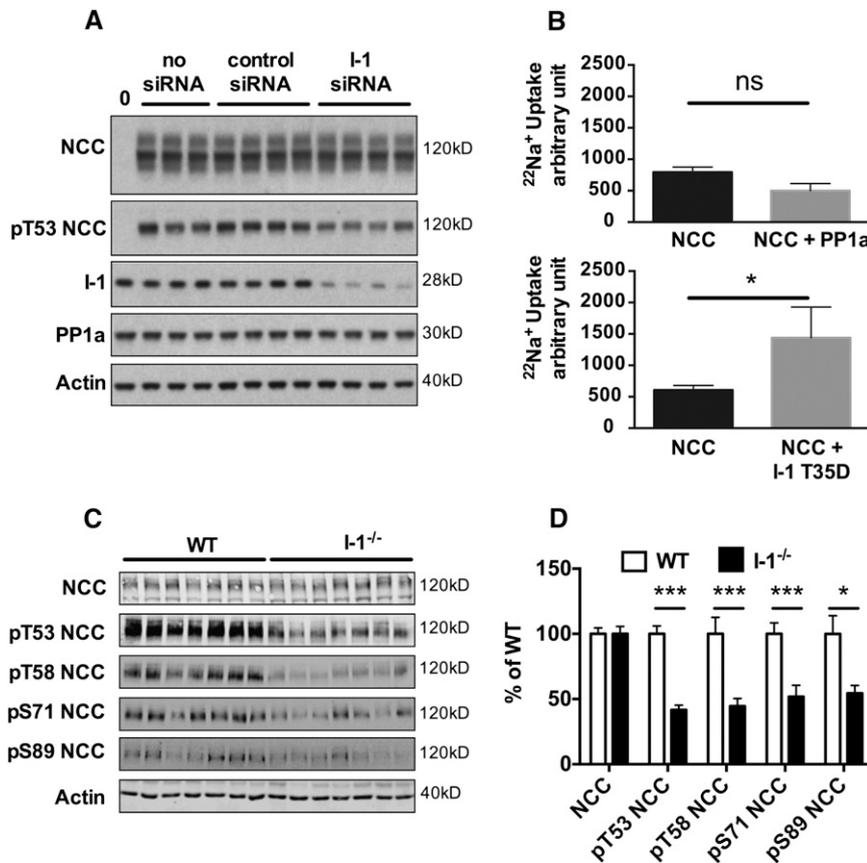
A

B

C

D

Figure 3. I-1 regulates NCC activity and phosphorylation. (A) Immunoblot analysis of HEK293 cells with tetracycline-inducible NCC overexpression (Flp-InNCC) reveals endogenous expression of I-1 and PP1a. Small interfering RNA (siRNA) knockdown of I-1 (I-1 siRNA) reduces endogenous I-1 protein abundance compared with no siRNA– and control siRNA–treated cells. Although the reduced I-1 abundance does not affect PP1a and total NCC abundance, it decreases NCC phosphorylation on threonine 53 (pT53 NCC). (B) Thiazide-sensitive ^{22}Na uptake was measured in oocytes overexpressing NCC. Coexpression of NCC with the catalytic subunit of PP1 (PP1a) does not significantly reduce thiazide-sensitive ^{22}Na uptake. Coexpression of NCC with constitutively active I-1 (I-1 T35D) profoundly stimulates thiazide-sensitive ^{22}Na uptake. Together, the data suggest that enhancing the basal level of phosphatase activity in the oocyte has little effect but that inhibiting this activity has a substantial effect; $n=3$ for each condition (mean±SEM); significance (by ANOVA) is shown (*$P<0.05$). (C) Immunoblot analysis of kidney membrane fractions from WT and I-1$^{-/-}$ mice was used to quantify the abundance of total NCC and NCC phosphorylated at threonine 53 (pT53 NCC), threonine 58 (pT58 NCC), serine 71 (pS71 NCC), and serine 89 (pS89 NCC). (D) Densitometric analysis from NCC immunoblots that were normalized to β-actin protein levels and expressed for I-1$^{-/-}$ mice in percent of control. Mean±SEM ($n=7$). Statistical significance was calculated with unpaired t test (*$P<0.05$; ***$P<0.001$).

natriuretic response to furosemide was even increased in I-1$^{-/-}$ mice (Figure 5D). Because I-1$^{-/-}$ mice have a lowered BP and an unchanged NKCC2 phosphorylation, this response is unlikely related to an increased NKCC2 function, but, rather, it is consistent with the reduced NCC activity in I-1$^{-/-}$ mice, which perhaps lowered the capacity of the DCT to absorb the furosemide-induced sodium load.

I-1 Deficiency Does Not Affect SPAK Phosphorylation

SPAK is thought to represent the final step in the WNK pathway controlling NCC phosphorylation. To test whether I-1 may interfere with the WNK/SPAK pathway, we analyzed the abundance, phosphorylation, and subcellular localization of SPAK in kidneys of WT and I-1$^{-/-}$ mice using antibodies directed against total SPAK and SPAK phosphorylated at Ser373. Neither the total abundance nor the phosphorylation level of SPAK was different between WT and I-1$^{-/-}$ mice, which were assessed by IB and IHC (Figure 6). Likewise, mRNA expression of the upstream SPAK regulators WNK4 and kidney-specific WNK1 were not different between genotypes (Supplemental Table 4).

DISCUSSION

The shortness and hidden localization of the DCT in the renal labyrinth complicate analyses of DCT function and underlying regulatory mechanisms. Using freehand microdissection, previous studies established transcriptome data for the renal distal convolution,[21,22] but the gradual transition from the DCT to the connecting tubule makes it almost impossible to precisely define the border between these functionally different segments. Moreover, the low yield of microdissection requires amplification of obtained cDNAs, which bears the risk of increased false-positive and false-negative results. In the present study, we combined the early DCT specificity of PV-EGFP expression with the high yield of COPAS to obtain rather pure DCT preparations on a large scale without the need for any further cDNA amplification. IB and transcriptomic analysis confirmed the high degree of purity of the isolated DCT samples. Differential hybridization and analysis of ALL, EGFP$^-$, and EGFP$^+$ tubules further confirmed the reliability of our approach and permitted us to identify DCT-enriched gene products. As expected, the known DCT-specific genes NCC, TRPM6, and PV showed the most significant enrichment in our DCT preparations. Other than these three strongly enriched genes, about 300 other genes were found to be more than 10-fold enriched in the DCT. Among these DCT-enriched genes are the known NCC regulators SPAK,[35]
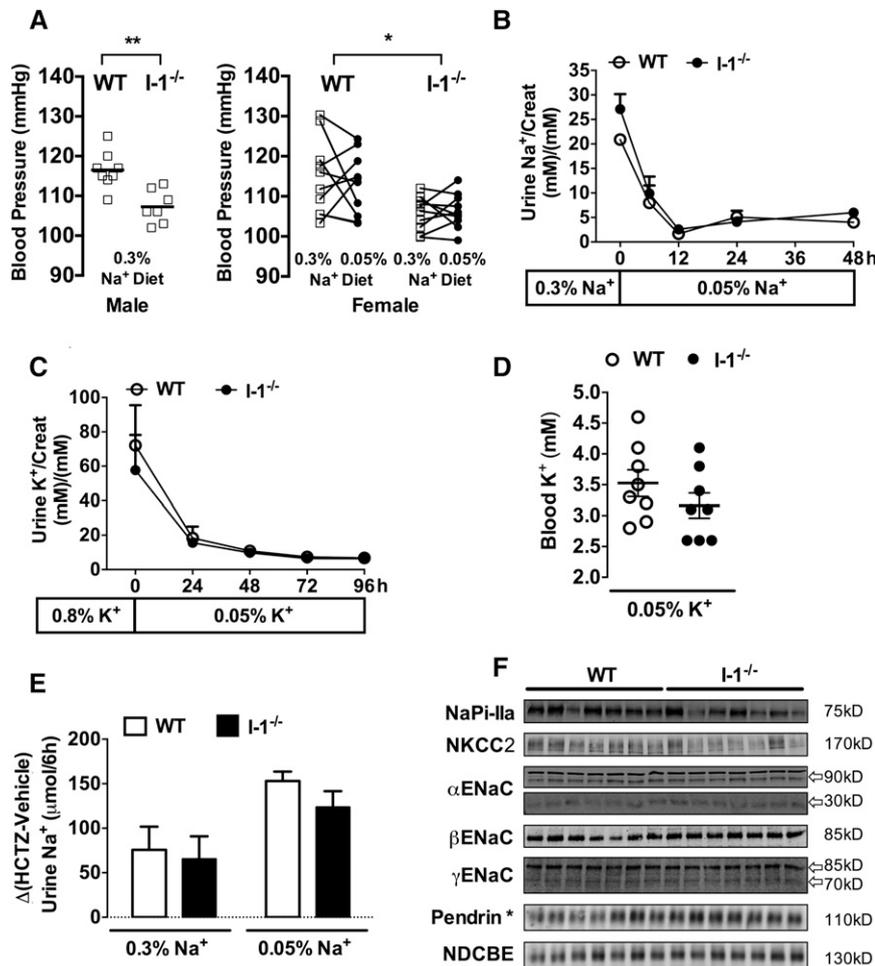
Figure 4. I-1 deficiency lowers arterial blood pressure but has little or no effect on Na$^+$, and K$^+$ diet adaptation, HCTZ response, and renal ion transporter abundances. (A) Systolic BP was measured with the tail-cuff method in WT and I-1$^{-/-}$ male and female mice on standard (0.3% Na$^+$; open square) or low (0.05% Na$^+$; filled circle) Na$^+$ diets. Measurements were done for 4 consecutive days. Each data point corresponds to an average of 4 days. Statistical analysis was performed using two-way ANOVA test for each dietary period (variables were the genotype and time). *$P<0.05$; **$P<0.01$ ($n=10$ per group). (B) Urine Na$^+$ excretion in WT and I-1$^{-/-}$ mice before and after the switch from standard to low Na$^+$ diet. No statistical difference was found between the two groups ($n=6$ per group). Urine Na$^+$ excretion was normalized to creatinine excretion. (C) Urine K$^+$ excretion in WT and I-1$^{-/-}$ mice before and after the switch from standard (0.8% K$^+$) to low (0.05% K$^+$) K$^+$ diet. No statistical differences were found between the two groups ($n=8$ per group). Urine K$^+$ excretion was normalized to creatinine excretion. (D) Plasma K$^+$ was measured after 4 days on low K$^+$ diet by blood sampling from the heart. Values are means±SEM. I-1$^{-/-}$ mice had slightly lower plasma K$^+$ values than WT mice, but a significant statistical difference was not reached ($P=0.24$, t test; $n=8$ per group). (E) Effect of HCTZ injection (50 mg/kg body wt intraperitoneally) on urinary Na$^+$ excretion in WT (open bars) and I-1$^{-/-}$ (filled bars) mice that were kept for 14 days on either standard or low Na$^+$ diet. Urines were collected for 6 hours after injection of either vehicle or HCTZ. The thiazide-sensitive component of urinary Na$^+$ excretion is presented as the difference between HCTZ- and vehicle-induced natriuresis within the first 6 hours postinjection. Data are shown as mean±SEM. No statistically significant difference between WT and I-1$^{-/-}$ was found ($P=0.79$ for standard Na$^+$; $P=0.08$ for low Na$^+$ diet, t test; $n=8-9$ mice in each group). (F) Immunoblot analysis of kidney membrane fractions from WT and I-1$^{-/-}$ mice showing the abundance of major apical Na$^+$ transporting pathways along the nephron. Densitometric

WNK4,[36] KS-WNK1,[30] and KLHL-3.[17,18] Interestingly, several of the other DCT-enriched genes are known to be involved in the control of cell growth and differentiation during development (*e.g.*, Sfrp1, Sox9, Lrrn1, Prox1, and Sall3). The high expression levels of these developmental genes in the adult DCT may relate to the particular structural plasticity of the DCT to growth stimuli.[37]

NCC is activated by phosphorylation through the WNK–SPAK pathway.[35] Usually, the activity of kinases is counterbalanced by phosphatases. Prior studies suggested that PP4 regulates NCC.[19] Here we report that PP1, PP2, and PP3 are also highly expressed in DCT cells. The specificity and catalytic activity of phosphatases are modulated by the interaction with specific regulatory and inhibitory subunits.[38] In this study, we identified the I-1 to be highly enriched in the mouse and human DCTs as well as the TAL. The latter is consistent with previous data that showed a localization of I-1 in the medullary and cortical TALs.[39,40] I-1 is also expressed in brain, skeletal muscle, and heart, where it is thought to contribute to synaptic plasticity,[41] muscle glycogen metabolism,[42] and cardiac contractility and excitability.[24] Using three independent experimental systems, we now provide evidence that I-1 also regulates renal NCC function. In *Xenopus laevis* oocytes, coexpression of I-1 and NCC profoundly increases thiazide-sensitive Na$^+$ uptake, whereas knockdown of I-1 in HEK293 cells as well as I-1 deficiency in mice led to a pronounced reduction in NCC phosphorylation. The similarity of the data in the HEK293 cells *in vitro* and the kidney *in vivo* indicates that the reduced NCC phosphorylation is a cell-autonomous effect of I-1 deficiency. We have recently shown that *ex vivo* incubation of DCTs with the PP1 and PP2a inhibitor calyculin A drastically increases NCC phosphorylation.[33] Given that I-1 is a rather specific inhibitor of PP1 with no effects

analysis was normalized to β-actin protein levels for each blot (Supplemental Tables 1–4). Statistical significance was calculated with t test (*$P<0.05$).

Table 1. Physiologic blood parameters in WT and I-1$^{-/-}$ littermates on a standard (0.3% Na$^+$) and low Na$^+$ (0.05% Na$^+$) diet

Parameter	Standard Diet			Low Na$^+$ Diet		
	WT	I-1$^{-/-}$	P Value	WT	I-1$^{-/-}$	P Value
pH	7.15±0.02 (9)	7.16±0.02 (8)	NS	7.15±0.02 (10)	7.17±0.02 (9)	NS
pCO$_2$ (mmHg)	56.74±2.31 (9)	55.16±3.72 (8)	NS	58.70±2.23 (10)	58.10±1.75 (9)	NS
HCO$_3^-$ (mM)	18.97±0.54 (9)	18.71±0.71 (8)	NS	19.74±0.67 (10)	20.44±0.63 (9)	NS
K$^+$ (mM)	3.40±0.14 (9)	3.30±0.11 (8)	NS	3.98±0.25 (10)	3.56±0.19 (9)	NS
Na$^+$ (mM)	142.57±0.57 (9)	142.22±0.52 (8)	NS	148.60±±.70 (10)	148.89±0.54 (9)	NS
Cl$^-$ (mM)	106.86±1.10 (9)	106.00±1.36 (8)	NS	112.40±0.99 (10)	110.67±0.53 (9)	NS
Ca^{2+} (mM)	0.73±0.06 (9)	0.73±0.08 (8)	NS	0.74±0.06 (10)	0.70±0.06 (9)	NS
Mg^{2+} (mM)	0.88±0.12 (4)	0.87±0.03 (4)	NS	ND	ND	
Aldosterone (ng/L)	402.43±35.13 (10)	505.99±61.23 (9)	NS	ND	ND	
Hematocrit (%)	44.7±0.8 (9)	43.8±0.8 (8)	NS	45.6±0.9 (10)	46.3±1.0 (9)	NS

Values are means±SEM. Statistical significance between WT and knockout on the same diet is assessed by unpaired t test. ND, not determined.

Table 2. Physiologic urinary parameters in WT and I-1$^{-/-}$ littermates on a standard (0.3% Na$^+$) and low Na$^+$ (0.05% Na$^+$) diet

Parameter	Standard Diet			Low Na$^+$ Diet		
	WT	I-1$^{-/-}$	P Value	WT	I-1$^{-/-}$	P Value
Urine volume (ml)	1.44±0.15 (9)	1.53±0.21 (9)	NS	1.26±0.21 (10)	1.60±0.22 (10)	NS
UNa$^+$/UCreat	28.19±1.39 (9)	32.22±1.45 (9)	NS	1.83±1.03 (6)	4.17±1.65 (8)	NS
UK$^+$/UCreat	165.5±27.6 (9)	181.8±27.2 (9)	NS	118.0±19.9 (9)	138.2±22.4 (10)	NS
UAldo/UCreat	3.76±2.53 (9)	4.29±1.11 (9)	NS	17.79±3.52 (7)	14.96±2.53 (10)	NS
UCa^{2+}/UCreat	0.289±0.058 (9)	0.320±0.045 (9)	NS	ND	ND	

Values are means±SEM. Statistical significance between WT and knockout on the same diet is assessed by unpaired t test. U, urinary; Creat, creatinine; Aldo, aldosterone; ND, not determined.

on PP2a and PP2b (also called PP3),[38] it is tempting to speculate that the observed effects of I-1 are mediated by PP1. Consistent with an involvement of PP1 in NCC regulation, preliminary yeast two-hybrid and coimmunoprecipitation data indicated that PP1 physically interacts with NCC (R.A.F., unpublished observations). In the oocyte expression system, PP1 was shown to also control NKCC1.[43] The effect on NKCC1 seemed to be mediated by both direct dephosporylation of the transporter and dephosphorylation of NKCC1-activating SPAK. In our study, we did not test by which mechanism I-1 controls NCC dephosphorylation, but the unchanged phosphorylation levels of SPAK1 in I-1$^{-/-}$ mice indicate that I-1 does not exert its effects through reducing phosphorylation and activation of the SPAK pathway.

Interestingly, although I-1 is also highly abundant in the TAL, I-1$^{-/-}$ mice do not show any significant effect on the phosphorylation levels of NKCC2. The TAL expresses it in addition to I-1 high levels of another endogenous PP1 inhibitor named DARPP-32 (Ppp1r1b),[39,40] which may compensate for the loss of I-1 in the TAL.

I-1 deficiency does not completely abrogate NCC phosphorylation in the kidney. The maintenance of a certain level of NCC phosphorylation may explain the rather mild phenotype of the I-1$^{-/-}$ mice. In contrast to patients with Gitelman syndrome and NCC-deficient mice as well as NCC knock-in mice bearing a Gitelman mutation (Ser707/X)[44] and SPAK-deficient mice,[45,46] the I-1$^{-/-}$ mice have no secondary hyperaldosteronism, hypomagnesaemia, and hypocalciuria. However, I-1$^{-/-}$ mice tend to have a reduced thiazide response on dietary Na$^+$ restriction and a trend for slightly lowered plasma K$^+$ concentrations. Moreover, they have a lower BP on standard and low Na$^+$ diet. As such, the phenotype resembles the one seen in SPAK$^{+/-}$ mice, which also have reduced NCC phosphorylation levels and arterial hypotension without any significant abnormalities for plasma and urine electrolytes, plasma aldosterone, and thiazide response.[46] Likewise, NCC$^{+/-}$ mice (D.L.-C., unpublished observation) and humans heterozygous for NCC mutations have low BP[47] without frank Gitelman disease.[48] Also, thiazides are known to efficiently reduce BP without provoking obvious extracellular volume depletion in many patients.[49] However, because I-1 is expressed in heart and arterial vessels, we cannot rule out that the lowered BP in I-1$^{-/-}$ mice is of extrarenal origin, although previous studies reported only rather small (if any) effects of I-1 deficiency on heart ejection fraction and no effects on aortic contractility.[50]

Another reason for the mild phenotype of I-1$^{-/-}$ mice could be rooted in the compensatory upregulation of other ion transporting pathways along the nephron. Previous studies suggest that NCC$^{-/-}$ mice compensate, in part, by activating the epithelial sodium channel ENaC.[51,52] Moreover, NCC$^{-/-}$ mice exhibit an enhanced abundance of the bicarbonate-chloride cotransporter pendrin,[53] which when deleted in NCC$^{-/-}$ mice, led to lethal salt wasting.[54] Consistent with the
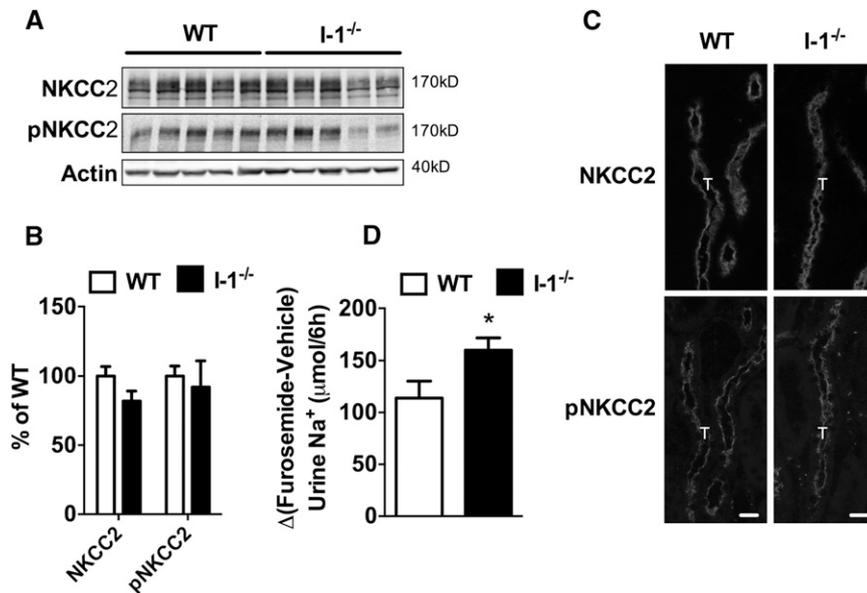
Figure 5. I-1 deficiency does not affect NKCC2 abundance and phosphorylation. (A) Immunoblot analysis of kidney membrane fractions from WT and I-1$^{-/-}$ mice for total NKCC2 and phosphorylated NKCC2 (pNKCC2). (B) Densitometric analysis was normalized to β-actin protein levels. No statistical difference was detected between groups (t test; n=5 per group). (C) Representative immunostainings for NKCC2 and pNKCC2 on consecutive cryosections of WT and I-1$^{-/-}$ mouse kidneys. NKCC2 and pNKCC2 are found in the apical membrane of the TAL (T). No differences are seen between WT and I-1$^{-/-}$ mice. Scale bars, ~20 μm. (D) Effect of furosemide injection (40 mg/kg body wt intraperitoneally) on urinary Na$^+$ excretion in WT (open bars) and I-1$^{-/-}$ (filled bars) mice. Urines were collected for 6 hours after injection of either vehicle or furosemide. The furosemide-sensitive component of urinary Na$^+$ excretion is presented as the difference between furosemide- and vehicle-induced natriuresis within the first 6 hours postinjection. Data are shown as mean±SEM (n=9 for each group). Statistical significance was assessed by t test (*$P<0.05$).

vitro and *in vivo*. Loss of I-1 expression lowers arterial BP without other cardinal features of complete NCC deficiency, such as hypokalemic alkalosis and hypomagnesemia. As such, I-1 deficiency resembles the phenotype seen in human heterozygotes for NCC mutations, which also have reduced BP,[47] but no other symptoms characteristic of Gitelman syndrome.[48] Because several patients with a full Gitelman phenotype have only one or even no alleles with NCC mutations, it might be interesting to analyze these patients for mutations in I-1 or other identified DCT-enriched genes. Thus, I-1 represents a new gene involved in regulation of NCC and BP that might be affected in hereditary and acquired renal tubulopathies.

CONCISE METHODS

Animals

For COPAS sorting, we used adult (10–12 weeks old) male and female PV-EGFP transgenic mice.[26] I-1–deficient mice were a gift from P. Greengard.[41] Both mouse strains were kept in a homogenetic C57BL/6J background. All mice were maintained on a standard rodent diet with free access to food and water. For diet experiments, mice were kept on semisynthetic diets (Sniff, Soest, Germany) with either low sodium (0.05% Na$^+$) or low potassium (0.05% K$^+$) concentrations. For the control groups, NaCl or KCl was supplemented to these diets to reach either standard sodium (0.3% Na$^+$) or standard potassium (0.8% K$^+$) contents. For blood sampling and organ harvesting, mice were anesthetized with a mixture of Ketamine (Narketan 10, 80 mg/kg body wt; Chassot, Belp, Switzerland) and Xylazine (Rompun, 33 mg/kg body wt; Bayer, Leverkusen, Germany). Daily urine sampling on different diets was performed in metabolic cages (Tecniplast, Buguggiate, Italy). Mice were kept on the diets for at least 14 days. All animal experiments were performed according to Swiss Animal Welfare laws, with approval of the local veterinary authority (Kantonales Veterinäramt Zürich).

COPAS Sorting and Microarray Analysis of Sorted DCT

Supplemental Materials and Methods has a detailed description of the protocol. COPAS sorting was adapted from the work by Miller *et al.*[23] The microarray data were deposited in the National Center for Biotechnology Information Gene Expression Omnibus database (accession number GSE51935).

Hydrochlorothiazide and Furosemide Treatment

WT and I-1$^{-/-}$ mice were kept for 14 days on 0.3% Na$^+$ or 0.05% Na$^+$ diet and then placed in metabolic cages. At day 4 in the metabolic

unchanged aldosterone levels in I-1$^{-/-}$ mice, we did not detect any evidence for an altered ENaC regulation. However, the pendrin protein abundance was found to be upregulated, which could have contributed to the compensated phenotype.

The inhibitory action of I-1 on PP1 depends on protein kinase A-mediated phosphorylation of I-1 at a threonine residue at position 35.[24,38] The DCT is target for several hormones that use cAMP and protein kinase A as signaling molecules.[55] Future work will have to establish how much I-1 participates in the hormonal control of NCC and which molecular mechanism might be involved. Moreover, it remains elusive if I-1 in the kidney also regulates the function of proteins other than NCC.

In conclusion, our study provides proof of concept that the search for DCT-enriched genes may reveal novel regulators of DCT and NCC function, although enrichment in the DCT does not necessarily mean that the gene product is of major importance and it may not have multiple functions and targets in the DCT cells. In this study, we identified the phosphatase inhibitor I-1 as a DCT-enriched gene product and a novel molecular player controlling the phosphorylation of NCC *in*
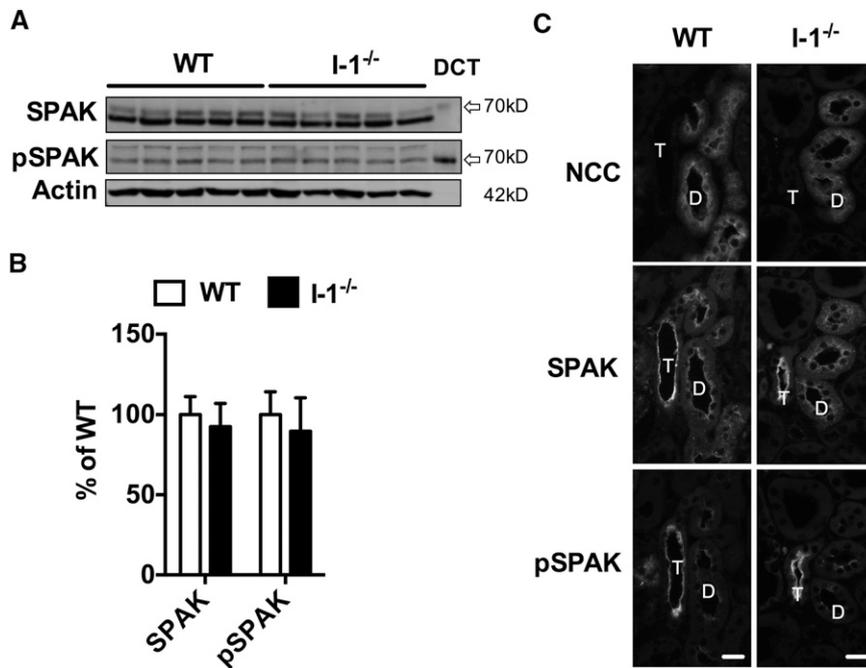
Figure 6. I-1 deficiency does not affect SPAK abundance and phosphorylation. (A) Immunoblot analysis of total kidney lysates from WT and I-1$^{-/-}$ mice for total SPAK and SPAK phosphorylated at Ser373 (pSPAK). Lysates from isolated DCTs were run in parallel and revealed SPAK and pSPAK at 70 kD. (B) Densitometric analysis was normalized to β-actin protein levels. No statistical difference between genotypes was detected with t test ($n=5$ mice per group). (C) Representative immunostainings for NCC, SPAK, and pSPAK on consecutive cryosections of WT and I-1$^{-/-}$ mouse kidneys. SPAK and pSPAK are clearly visible in NCC-negative TAL (T) and NCC-positive DCT (D). No differences are seen between WT and I-1$^{-/-}$ mice. Scale bars, ~20 μm.

cage, each mouse received a single intraperitoneal injection of vehicle (1:1 mixture of 0.9% NaCl solution with methanol or polyethylenglycol 300 for 0.3% Na$^+$ or 0.05% Na$^+$ diet, respectively), and urine was collected for the next 6 hours; 24 hours later, mice received either HCTZ (50 mg/kg; Sigma-Aldrich) or furosemide (Furo, 40 mg/kg; Sigma-Aldrich), and urine was collected again for a 6-hour period.

Biochemical Measurements
Blood gas and blood ions were measured with the ABL825Flex Blood Gas Analyzer (Radiometer, Copenhagen, Denmark). Blood magnesium was measured by atomic absorption spectrophotometry (PerkinElmer Apparatus, Model 3110; PerkinElmer, Cortabeuf, France). Plasma and urine aldosterone levels were measured with a radioimmunoassay using commercially available kits (DRG Diagnostics, Marburg, Germany, and DPC Dade Behring, La Défense, France, respectively). Urinary creatinine was assessed by the Jaffe method. Urinary electrolytes (Na$^+$, K$^+$, and Ca^{2+}) were measured by ion chromatography (Metrohm Ion Chromatograph, Herisau, Switzerland).

BP Recordings
Systolic BP was recorded on conscious mice using the noninvasive tail-cuff method (Visitech). Mice were habituated to the instrument for 4 consecutive days. Then, BP was measured daily between 10:00 and

12:00 AM for 5 consecutive days. At least 20 subsequent BP recordings were taken and averaged for each mouse. The average values per mouse and per day were used to calculate a mean systolic BP per mouse for 4 consecutive days.

IHC
Mouse kidneys were fixed by vascular perfusion of 3% paraformaldehyde in phosphate buffer and processed for immunohistochemistry as described.[56] Human kidney samples were archived tissue. Cryosections were analyzed with a Leica fluorescence microscope. Cryosections were examined with a fluorescence microscope (Leica DM6000B). Images were acquired with a charge-coupled device camera and processed by Adobe Photoshop CS3.

IB
Membrane protein fractions were prepared, resolved on SDS polyacrylamide gels, and blotted on nitrocellulose membranes.[57] Binding of the primary antibody was visualized using Infra Red Dye–conjugated secondary antibodies (LI-COR Biosciences) and an Odyssey infrared-scanner detection system (LI-COR Biosciences).

Antibodies
Primary and secondary antibodies were diluted for IHC and IB in PBS with 0.1% BSA and LI-COR Blocking Buffer, respectively. Antibodies used were rabbit anti–I-1 (IHC: 1/1000, IB: 1/20,000; Epitomics), rabbit anti–NaPi-IIa (IB: 1/5000),[58] rabbit anti-NKCC2 (IB: 1/10,000),[56] rabbit anti-total NCC[27] (IHC: 1/8000), rabbit anti-total NCC[58] (IB: 1/2000), rabbit anti–phospho-Thr53 NCC[57] (IB: 1/5000), rabbit anti–phospho-Thr58 NCC[58] (IB: 1/5000), rabbit anti–phospho-Ser71 NCC[58] (IB: 1/10,000), rabbit anti–phospho-Ser89 NCC[58] (IB: 1/10,000), mouse anti-CB28K (IHC: 1/20,000; Swant, Bellinzona, Switzerland), rabbit anti-αENaC[58] (IHC and IB: 1/10,000), rabbit anti-βENaC (IB: 1/40,000)[56], anti-γENaC[56] (IB: 1/20,000), rabbit anti-pendrin[59] (IB: 1/5000), rabbit anti–sodium-driven bicarbonate-chloride exchanger[60] (IB: 1/500), rabbit anti-SPAK (IHC and IB: 1/500, 07–2271; Milipore), and rabbit anti-human phospho-SPAK (Ser373; IHC and IB: 1/500, 07–2273; Milipore). For detection of phosphorylated NKCC2, we used a novel rabbit phosphoform-specific antibody (IHC and IB: 1/500). The antiserum against rat NKCC2 phosphorylated at T96 and T101 was generated by immunizing rabbits with the following phosphorylated peptide: QT^{P}FGHNT^{P}MC by Genscript. The C-terminal cysteine was added for conjugation to carrier protein and attachment of the peptide to the affinity purification column for subsequent affinity purification of the antisera against the phospho- and the corresponding nonphosphopeptide. Secondary antibodies were goat anti-rabbit IgG coupled to Alexa 555 dye (1/2000; Invitrogen), goat anti-mouse IgG coupled

to Alexa 488 dye (1/1000; Molecular Probes), and donkey anti-sheep IgG coupled to IRDye 800CW (1/20,000; Rockland, Gilbertsville, PA). The characterization of the novel antibody against phosphory-lated NKCC2 is shown in Supplemental Figure 2. The specificity of the antibodies for phosphorylated NCC forms was confirmed by de-phosphorylation of tissue homogenates and using kidneys of NCC-deficient mice as negative controls (Supplemental Figure 3). The SPAK and pSPAK antibodies were characterized by comparing their binding patterns with total lysates of isolated DCTs and whole-mouse kidneys. The phosphoform specificity of the pSPAK antibody was confirmed by using dephosphorylated kidney protein homogenates (Supplemental Figure 4).

HEK293 Cells with Inducible NCC Expression Cells

The Flp-In T-REx HEK NCC cell line, which was described pre-viously,[8] is maintained in high-glucose DMEM containing 10% vol/vol FBS, 200 μg/ml hygromycin, 15 μg/ml blasticidin, and penicillin/streptomycin. NCC is induced by incubating the cells with tetracy-cline (1 μg/ml) followed by cell lysis and IB. To knock down endogenous I-1 expression, HEK cells were transfected using Lipofectamine 2000 (Invitrogen) with 20–40 nM I-1 small interfering RNA oligonucleotides (5′-CCACATCTAAGTCCACTT; Invitrogen) according to the manu-facturer's protocol.

Oocyte Experiments

The uptake of ^{22}Na was performed as described previously.[61] T7 RNA polymerase (mMESSAGE mMACHINE; Ambion) was used to make cRNA. Sorted *Xenopus* oocytes were injected with 50 nl water con-taining 5 ng NCC with or without 5 ng PP1a and constitutive active I-1 (ppp1r1a) T35D variant, which is noted in the figures. For each experimental condition, 10–20 oocytes were injected; 3 days after in-jection, oocytes were incubated in chloride-free medium for 3–4 hours at 18°C before Na uptake was measured. The *n* value given in the figures represents the number of independent experiments.

REFERENCES

1. Reilly RF, Ellison DH: Mammalian distal tubule: Physiology, patho-physiology, and molecular anatomy. *Physiol Rev* 80: 277–313, 2000
2. Gamba G: The thiazide-sensitive Na+-Cl- cotransporter: Molecular bi-ology, functional properties, and regulation by WNKs. *Am J Physiol Renal Physiol* 297: F838–F848, 2009
3. Simon DB, Nelson-Williams C, Bia MJ, Ellison D, Karet FE, Molina AM, Vaara I, Iwata F, Cushner HM, Koolen M, Gainza FJ, Gitleman HJ, Lifton RP: Gitelman's variant of Bartter's syndrome, inherited hypokalaemic alkalosis, is caused by mutations in the thiazide-sensitive Na-Cl co-transporter. *Nat Genet* 12: 24–30, 1996
4. Wilson FH, Disse-Nicodème S, Choate KA, Ishikawa K, Nelson-Williams C, Desitter I, Gunel M, Milford DV, Lipkin GW, Achard JM, Feely MP, Dussol B, Berland Y, Unwin RJ, Mayan H, Simon DB, Farfel Z, Jeunemaitre X, Lifton RP: Human hypertension caused by mutations in WNK kinases. *Science* 293: 1107–1112, 2001
5. Yu Z, Serra A, Sauter D, Loffing J, Ackermann D, Frey FJ, Frey BM, Vogt B: Sodium retention in rats with liver cirrhosis is associated with in-creased renal abundance of NaCl cotransporter (NCC). *Nephrol Dial Transplant* 20: 1833–1841, 2005
6. Song J, Knepper MA, Verbalis JG, Ecelbarger CA: Increased renal ENaC subunit and sodium transporter abundances in streptozotocin-induced type 1 diabetes. *Am J Physiol Renal Physiol* 285: F1125–F1137, 2003
7. Mu S, Shimosawa T, Ogura S, Wang H, Uetake Y, Kawakami-Mori F, Marumo T, Yatomi Y, Geller DS, Tanaka H, Fujita T: Epigenetic modu-lation of the renal β-adrenergic-WNK4 pathway in salt-sensitive hy-pertension. *Nat Med* 17: 573–580, 2011
8. Hoorn EJ, Walsh SB, McCormick JA, Fürstenberg A, Yang CL, Roeschel T, Paliege A, Howie AJ, Conley J, Bachmann S, Unwin RJ, Ellison DH: The calcineurin inhibitor tacrolimus activates the renal sodium chloride cotransporter to cause hypertension. *Nat Med* 17: 1304–1309, 2011
9. Davis BR, Cutler JA, Gordon DJ, Furberg CD, Wright JT Jr., Cushman WC, Grimm RH, LaRosa J, Whelton PK, Perry HM, Alderman MH, Ford CE, Oparil S, Francis C, Proschan M, Pressel S, Black HR, Hawkins CM;

ALLHAT Research Group: Rationale and design for the Antihypertensive and Lipid Lowering Treatment to Prevent Heart Attack Trial (ALLHAT). *Am J Hypertens* 9: 342–360, 1996

10. Bergaya S, Vidal-Petiot E, Jeunemaitre X, Hadchouel J: Pathogenesis of pseudohypoaldosteronism type 2 by WNK1 mutations. *Curr Opin Nephrol Hypertens* 21: 39–45, 2012

11. Uchida S: Pathophysiological roles of WNK kinases in the kidney. *Pflugers Arch* 460: 695–702, 2010

12. Welling PA, Chang YP, Delpire E, Wade JB: Multigene kinase network, kidney transport, and salt in essential hypertension. *Kidney Int* 77: 1063–1069, 2010

13. Belge H, Gailly P, Schwaller B, Loffing J, Debaix H, Riveira-Munoz E, Beauwens R, Devogelaer JP, Hoenderop JG, Bindels RJ, Devuyst O: Renal expression of parvalbumin is critical for NaCl handling and response to diuretics. *Proc Natl Acad Sci U S A* 104: 14849–14854, 2007

14. Arroyo JP, Lagnaz D, Ronzaud C, Vázquez N, Ko BS, Moddes L, Ruffieux-Daidié D, Hausel P, Koesters R, Yang B, Stokes JB, Hoover RS, Gamba G, Staub O: Nedd4-2 modulates renal Na$^+$-Cl$^-$ cotransporter via the aldosterone-SGK1-Nedd4-2 pathway. *J Am Soc Nephrol* 22: 1707–1719, 2011

15. Fejes-Tóth G, Frindt G, Náray-Fejes-Tóth A, Palmer LG: Epithelial Na$^+$ channel activation and processing in mice lacking SGK1. *Am J Physiol Renal Physiol* 294: F1298–F1305, 2008

16. Rozansky DJ, Cornwall T, Subramanya AR, Rogers S, Yang YF, David LL, Zhu X, Yang CL, Ellison DH: Aldosterone mediates activation of the thiazide-sensitive Na-Cl cotransporter through an SGK1 and WNK4 signaling pathway. *J Clin Invest* 119: 2601–2612, 2009

17. Boyden LM, Choi M, Choate KA, Nelson-Williams CJ, Farhi A, Toka HR, Tikhonova IR, Bjornson R, Mane SM, Colussi G, Lebel M, Gordon RD, Semmekrot BA, Poujol A, Välimäki MJ, De Ferrari ME, Sanjad SA, Gutkin M, Karet FE, Tucci JR, Stockigt JR, Keppler-Noreuil KM, Porter CC, Anand SK, Whiteford ML, Davis ID, Dewar SB, Bettinelli A, Fadrowski JJ, Belsha CW, Hunley TE, Nelson RD, Trachtman H, Cole TR, Pinsk M, Bockenhauer D, Shenoy M, Vaidyanathan P, Foreman JW, Rasoulpour M, Thameem F, Al-Shahrouri HZ, Radhakrishnan J, Gharavi AG, Goilav B, Lifton RP: Mutations in kelch-like 3 and cullin 3 cause hypertension and electrolyte abnormalities. *Nature* 482: 98–102, 2012

18. Louis-Dit-Picard H, Barc J, Trujillano D, Miserey-Lenkei S, Bouatia-Naji N, Pylypenko O, Beaurain G, Bonnefond A, Sand O, Simian C, Vidal-Petiot E, Soukaseum C, Mandet C, Broux F, Chabre O, Delahousse M, Esnault V, Fiquet B, Houillier P, Bagnis CI, Koenig J, Konrad M, Landais P, Mourani C, Niaudet P, Probst V, Thauvin C, Unwin RJ, Soroka SD, Ehret G, Ossowski S, Caulfield M, Bruneval P, Estivill X, Froguel P, Hadchouel J, Schott JJ, Jeunemaitre X: KLHL3 mutations cause familial hyperkalemic hypertension by impairing ion transport in the distal nephron. *Nat Genet* 44: 456–460, 2012

19. Glover M, Mercier Zuber A, Figg N, O'Shaughnessy KM: The activity of the thiazide-sensitive Na(+)-Cl(-) cotransporter is regulated by protein phosphatase PP4. *Can J Physiol Pharmacol* 88: 986–995, 2010

20. Chabardès-Garonne D, Méjean A, Aude JC, Cheval L, Di Stefano A, Gaillard MC, Imbert-Teboul M, Wittner M, Balian C, Anthouard V, Robert C, Ségurens B, Wincker P, Weissenbach J, Doucet A, Elalouf JM: A panoramic view of gene expression in the human kidney. *Proc Natl Acad Sci U S A* 100: 13710–13715, 2003

21. Cheval L, Pierrat F, Dossat C, Genete M, Imbert-Teboul M, Duong Van Huyen JP, Poulain J, Wincker P, Weissenbach J, Piquemal D, Doucet A: Atlas of gene expression in the mouse kidney: New features of glomerular parietal cells. *Physiol Genomics* 43: 161–173, 2011

22. Pradervand S, Zuber Mercier A, Centeno G, Bonny O, Firsov D: A comprehensive analysis of gene expression profiles in distal parts of the mouse renal tubule. *Pflugers Arch* 460: 925–952, 2010

23. Miller RL, Zhang P, Chen T, Rohrwasser A, Nelson RD: Automated method for the isolation of collecting ducts. *Am J Physiol Renal Physiol* 291: F236–F245, 2006

24. Wittköpper K, Dobrev D, Eschenhagen T, El-Armouche A: Phosphatase-1 inhibitor-1 in physiological and pathological β-adrenoceptor signalling. *Cardiovasc Res* 91: 392–401, 2011

25. Cohen PT: Protein phosphatase 1—targeted in many directions. *J Cell Sci* 115: 241–256, 2002

26. Meyer AH, Katona I, Blatow M, Rozov A, Monyer H: In vivo labeling of parvalbumin-positive interneurons and analysis of electrical coupling in identified neurons. *J Neurosci* 22: 7055–7064, 2002

27. Loffing J, Loffing-Cueni D, Valderrabano V, Kläusli L, Hebert SC, Rossier BC, Hoenderop JG, Bindels RJ, Kaissling B: Distribution of transcellular calcium and sodium transport pathways along mouse distal nephron. *Am J Physiol Renal Physiol* 281: F1021–F1027, 2001

28. Voets T, Nilius B, Hoefs S, van der Kemp AW, Droogmans G, Bindels RJ, Hoenderop JG: TRPM6 forms the Mg2+ influx channel involved in intestinal and renal Mg2+ absorption. *J Biol Chem* 279: 19–25, 2004

29. Ellison DH, Biemesderfer D, Morrisey J, Lauring J, Desir GV: Immunocytochemical characterization of the high-affinity thiazide diuretic receptor in rabbit renal cortex. *Am J Physiol* 264: F141–F148, 1993

30. Yang CL, Angell J, Mitchell R, Ellison DH: WNK kinases regulate thiazide-sensitive Na-Cl cotransport. *J Clin Invest* 111: 1039–1045, 2003

31. Chen G, Zhou X, Florea S, Qian J, Cai W, Zhang Z, Fan GC, Lorenz J, Hajjar RJ, Kranias EG: Expression of active protein phosphatase 1 inhibitor-1 attenuates chronic beta-agonist-induced cardiac apoptosis. *Basic Res Cardiol* 105: 573–581, 2010

32. Wu JQ, Guo JY, Tang W, Yang CS, Freel CD, Chen C, Nairn AC, Kornbluth S: PP1-mediated dephosphorylation of phosphoproteins at mitotic exit is controlled by inhibitor-1 and PP1 phosphorylation. *Nat Cell Biol* 11: 644–651, 2009

33. Sorensen MV, Grossmann S, Roesinger M, Gresko N, Todkar AP, Barmettler G, Ziegler U, Odermatt A, Loffing-Cueni D, Loffing J: Rapid dephosphorylation of the renal sodium chloride cotransporter in response to oral potassium intake in mice. *Kidney Int* 83: 811–824, 2013

34. Morris RG, Hoorn EJ, Knepper MA: Hypokalemia in a mouse model of Gitelman's syndrome. *Am J Physiol Renal Physiol* 290: F1416–F1420, 2006

35. Richardson C, Rafiqi FH, Karlsson HK, Moleleki N, Vandewalle A, Campbell DG, Morrice NA, Alessi DR: Activation of the thiazide-sensitive Na$^+$-Cl$^-$ cotransporter by the WNK-regulated kinases SPAK and OSR1. *J Cell Sci* 121: 675–684, 2008

36. Lalioti MD, Zhang J, Volkman HM, Kahle KT, Hoffmann KE, Toka HR, Nelson-Williams C, Ellison DH, Flavell R, Booth CJ, Lu Y, Geller DS, Lifton RP: Wnk4 controls blood pressure and potassium homeostasis via regulation of mass and activity of the distal convoluted tubule. *Nat Genet* 38: 1124–1132, 2006

37. Kaissling B, Loffing J: Cell growth and cell death in renal distal tubules, associated with diuretic treatment. *Nephrol Dial Transplant* 13: 1341–1343, 1998

38. Cohen P: The structure and regulation of protein phosphatases. *Annu Rev Biochem* 58: 453–508, 1989

39. Meister B, Fryckstedt J, Schalling M, Cortés R, Hökfelt T, Aperia A, Hemmings HC Jr, Nairn AC, Ehrlich M, Greengard P: Dopamine- and cAMP-regulated phosphoprotein (DARPP-32) and dopamine DA1 agonist-sensitive Na$^+$,K$^+$-ATPase in renal tubule cells. *Proc Natl Acad Sci U S A* 86: 8068–8072, 1989

40. Fryckstedt J, Aperia A, Snyder G, Meister B: Distribution of dopamine- and cAMP-dependent phosphoprotein (DARPP-32) in the developing and mature kidney. *Kidney Int* 44: 495–502, 1993

41. Allen PB, Hvalby O, Jensen V, Errington ML, Ramsay M, Chaudhry FA, Bliss TV, Storm-Mathisen J, Morris RG, Andersen P, Greengard P: Protein phosphatase-1 regulation in the induction of long-term potentiation: Heterogeneous molecular mechanisms. *J Neurosci* 20: 3537–3543, 2000

42. Nimmo GA, Cohen P: The regulation of glycogen metabolism. Purification and characterisation of protein phosphatase inhibitor-1 from rabbit skeletal muscle. *Eur J Biochem* 87: 341–351, 1978

43. Gagnon KB, Delpire E: Multiple pathways for protein phosphatase 1 (PP1) regulation of Na-K-2Cl cotransporter (NKCC1) function: The N-terminal tail of the Na-K-2Cl cotransporter serves as a regulatory scaffold for Ste20-related proline/alanine-rich kinase (SPAK) AND PP1. *J Biol Chem* 285: 14115–14121, 2010

44. Yang SS, Lo YF, Yu IS, Lin SW, Chang TH, Hsu YJ, Chao TK, Sytwu HK, Uchida S, Sasaki S, Lin SH: Generation and analysis of the thiazide-sensitive Na+ -Cl- cotransporter (Ncc/Slc12a3) Ser707X knockin mouse as a model of Gitelman syndrome. *Hum Mutat* 31: 1304–1315, 2010

45. McCormick JA, Mutig K, Nelson JH, Saritas T, Hoorn EJ, Yang CL, Rogers S, Curry J, Delpire E, Bachmann S, Ellison DH: A SPAK isoform switch modulates renal salt transport and blood pressure. *Cell Metab* 14: 352–364, 2011

46. Yang SS, Lo YF, Wu CC, Lin SW, Yeh CJ, Chu P, Sytwu HK, Uchida S, Sasaki S, Lin SH: SPAK-knockout mice manifest Gitelman syndrome and impaired vasoconstriction. *J Am Soc Nephrol* 21: 1868–1877, 2010

47. Ji W, Foo JN, O'Roak BJ, Zhao H, Larson MG, Simon DB, Newton-Cheh C, State MW, Levy D, Lifton RP: Rare independent mutations in renal salt handling genes contribute to blood pressure variation. *Nat Genet* 40: 592–599, 2008

48. Cruz DN, Simon DB, Nelson-Williams C, Farhi A, Finberg K, Burleson L, Gill JR, Lifton RP: Mutations in the Na-Cl cotransporter reduce blood pressure in humans. *Hypertension* 37: 1458–1464, 2001

49. Ellison DH, Loffing J: Thiazide effects and adverse effects: Insights from molecular genetics. *Hypertension* 54: 196–202, 2009

50. Carr AN, Sutliff RL, Weber CS, Allen PB, Greengard P, de Lanerolle P, Kranias EG, Paul RJ: Is myosin phosphatase regulated in vivo by inhibitor-1? Evidence from inhibitor-1 knockout mice. *J Physiol* 534: 357–366, 2001

51. Brooks HL, Sorensen AM, Terris J, Schultheis PJ, Lorenz JN, Shull GE, Knepper MA: Profiling of renal tubule Na+ transporter abundances in NHE3 and NCC null mice using targeted proteomics. *J Physiol* 530: 359–366, 2001

52. Loffing J, Vallon V, Loffing-Cueni D, Aregger F, Richter K, Pietri L, Bloch-Faure M, Hoenderop JG, Shull GE, Meneton P, Kaissling B: Altered renal distal tubule structure and renal Na(+) and Ca(2+) handling in a mouse model for Gitelman's syndrome. *J Am Soc Nephrol* 15: 2276–2288, 2004

53. Vallet M, Picard N, Loffing-Cueni D, Fysekidis M, Bloch-Faure M, Deschênes G, Breton S, Meneton P, Loffing J, Aronson PS, Chambrey R, Eladari D: Pendrin regulation in mouse kidney primarily is chloride-dependent. *J Am Soc Nephrol* 17: 2153–2163, 2006

54. Soleimani M, Barone S, Xu J, Shull GE, Siddiqui F, Zahedi K, Amlal H: Double knockout of pendrin and Na-Cl cotransporter (NCC) causes severe salt wasting, volume depletion, and renal failure. *Proc Natl Acad Sci U S A* 109: 13368–13373, 2012

55. Morel F: Sites of hormone action in the mammalian nephron. *Am J Physiol* 240: F159–F164, 1981

56. Wagner CA, Loffing-Cueni D, Yan Q, Schulz N, Fakitsas P, Carrel M, Wang T, Verrey F, Geibel JP, Giebisch G, Hebert SC, Loffing J: Mouse model of type II Bartter's syndrome. II. Altered expression of renal sodium- and water-transporting proteins. *Am J Physiol Renal Physiol* 294: F1373–F1380, 2008

57. Sorensen MV, Grossmann S, Roesinger M, Gresko N, Todkar AP, Barmettler G, Ziegler U, Odermatt A, Loffing-Cueni D, Loffing J: Rapid dephosphorylation of the renal NaCl cotransporter in response to oral K+ intake. *Kidney Int* 83: 811–824, 2013

58. Custer M, Lötscher M, Biber J, Murer H, Kaissling B: Expression of Na-P (i) cotransport in rat kidney: Localization by RT-PCR and immunohistochemistry. *Am J Physiol* 266: F767–F774, 1994

59. Wagner CA, Finberg KE, Stehberger PA, Lifton RP, Giebisch GH, Aronson PS, Geibel JP: Regulation of the expression of the Cl-/anion exchanger pendrin in mouse kidney by acid-base status. *Kidney Int* 62: 2109–2117, 2002

60. Leviel F, Hübner CA, Houillier P, Morla L, El Moghrabi S, Brideau G, Hassan H, Parker MD, Kurth I, Kougioumtzes A, Sinning A, Pech V, Riemondy KA, Miller RL, Hummler E, Shull GE, Aronson PS, Doucet A, Wall SM, Chambrey R, Eladari D: The Na+-dependent chloride-bicarbonate exchanger SLC4A8 mediates an electroneutral Na+ reabsorption process in the renal cortical collecting ducts of mice. *J Clin Invest* 120: 1627–1635, 2010

61. Yang CL, Zhu X, Ellison DH: The thiazide-sensitive Na-Cl cotransporter is regulated by a WNK kinase signaling complex. *J Clin Invest* 117: 3403–3411, 2007